

EMI Analysis of DVI Link Connectors

Abhishek Patnaik, *Student Member, IEEE*, Soumya De, *Member, IEEE*, Yao-Jiang Zhang, *Member, IEEE*, James L. Drewniak, *Fellow, IEEE*, Chen Wang, Charles Jackson David Pommerenke, *Fellow, IEEE*,

Abstract—Electromagnetic interference (EMI) is correlated to mode conversion, from differential-mode signals to common-mode currents and further to antenna-mode currents on the outside of cables or enclosures. This paper presents methods to quantify the mode conversion caused by discontinuities in the digital visual interface (DVI) signal link. These discontinuities are mostly present in the DVI connector, the DVI cable, and the connector-cable interface. A systematic approach was developed in this study to isolate and identify the different coupling paths in a high-speed interface (in this case, DVI is shown), and also to identify which discontinuity is most critical to mitigate EMI. The method developed in this study can be used for any high-speed interface in modern communication systems.

Index Terms—Electromagnetic interference (EMI), coupling path, mode conversion, differential mode, common mode, antenna mode, cable shielding, port voltage, cable radiation, DVI, HDMI.

I. INTRODUCTION

THE digital visual interface (DVI) uses a high-speed serial link called transition minimized differential signaling (TMDS) to transmit signals between the CPU and the monitor using a DVI cable [1]. The DVI signal driver may drive both differential-mode (DM) and common-mode (CM) currents. The DM currents may give rise to CM currents when they encounter discontinuities along its path such as traces, DVI connector, load end terminations, etc. Fig. 1 illustrates different currents on a cable, wherein both DM and CM currents flowing along the differential pair signal lines are shown (black and green arrows). The CM return current (blue arrows) flows through the inner surface of the shielding braid. Antenna mode (AM) currents (red arrows) are those currents that flow on the outside of larger metal parts, causing EMI.

The term “antenna mode currents” was selected to distinguish between the “common-mode currents” that do not cause EMI (e.g., the CM return current inside the shielded cable), and the CM return currents that cause EMI (e.g., the fraction of the CM return current that flows on the outside of a shielded cable).

The DVI connector is partially inside and partially outside the computer chassis or enclosure. The DVI connector has certain structural imperfections that play a significant role in the leakage of internal energy of the system to appear outside and cause EMI problems. Fig. 2 shows the current flow in a typical DVI connector. The discontinuities along the signal

Manuscript received XXX, revised XXX. This work was supported in part by the National Science Foundation (NSF) under Grant IIP-1440110.

A. Patnaik, S. De, Y. Zhang, D. Pommerenke, J. Drewniak are with the EMC Laboratory, Missouri University of Science and Technology, Rolla, MO 65409, USA. Email: ap437@mst.edu, sdwt2@mst.edu, zhang.yaojiang@huawei.edu, davidjp@mst.edu, drewniak@mst.edu.

C. Jackson, C. Wang are with NVIDIA Corporation, Santa Clara, CA 95050, USA. Email: cjackson@nvidia.com, chenwang@nvidia.com.

Digital Object Identifier 10.1109/TEMC.2017.2702707

0018-9375 © 2017 IEEE. Personal use is permitted, but republication/redistribution requires IEEE permission.
[See http://www.ieee.org/publications_standards/publications/rights/index.html](http://www.ieee.org/publications_standards/publications/rights/index.html) for more information.

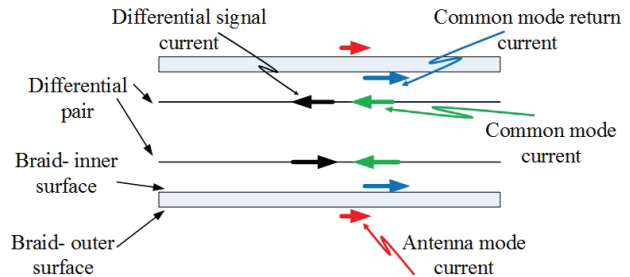


Fig. 1. Cable current definitions.

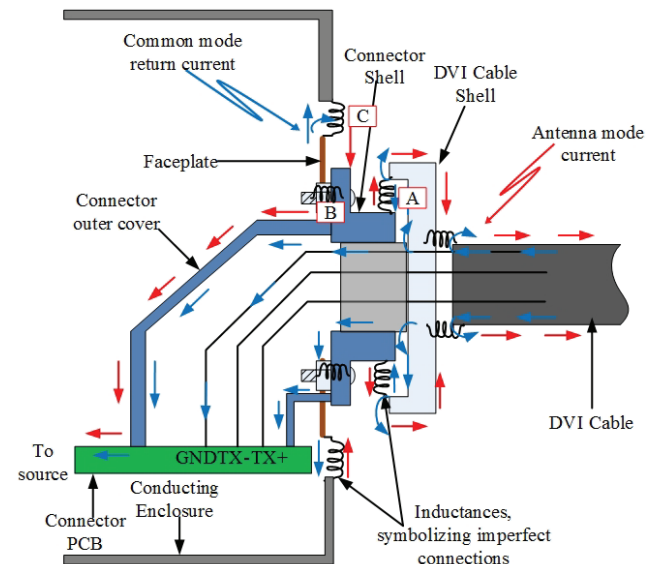


Fig. 2. DVI Connector-cable system.

link, such as the connector body shell gaps, gaps between the connector shell and the DVI cable shell (Fig. 2 A), DVI connector shell and bracket (Fig. 2 B) as well as the gaps between the connector and the CPU enclosure (Fig. 2 C), are the main reasons for mode conversion [2], [3], [4]. Voltages across these gaps are created by detours of the return currents. This implies that the connector imperfections drive AM currents on the DVI cable and enclosure. It is important to identify the different mode-conversion mechanisms and quantify the impact of the imperfections in the DVI signal link towards EMI. The connector investigated in this study is a dual stack DVI connector housed in a back shell also referred to as the connector shell or cover (Fig. 2). The main purpose of the connector shell is to provide a continuous closed conductive envelope for shielding. Ideally, this shell should make a 360° electrical contact with the outer supporting metallic bracket

enclosure system. However, it is very difficult to achieve such a perfect shield from a manufacturing, cost, and assembly point of view. Therefore, the connector body shell has certain apertures as well as a few contact points with the bracket. Each aperture reduces the shielding efficiency which results in increased emissions as electromagnetic energy can leak through these apertures. Many studies have shown how the apertures on the shield of a high-speed connector can hamper the shielding effectiveness of a connector [5], [6], [7]. The connector shell should also contact the enclosure of the entire system. Low impedance contacts are also needed for the other transitions such as the connector-shell and cable-shell assembly [8], [9]. These crucial contacts in the connector-enclosure-cable system can be represented as equivalent inductances [10].

In this paper, a systematic approach is proposed to study the important coupling paths and contacts/imperfections in the DVI signal link. The idea was to break the system into different blocks and quantify their impact towards the overall EMI. In the process, a transfer function was derived which relates the DM current from the source driver to AM current on the DVI cable which is further used to estimate the radiated field strengths. The impact of each block is quantified in the radiated field. The system is divided into different blocks such as:

- 1) The connector
- 2) The connector-cable assembly
 - a) The cable
 - b) The connector-cable system
- 3) Adjacent connectors

In this paper, only 1) and 2) are quantified. The coupling to adjacent connectors 3) is studied and quantified by the authors in an earlier study [11]. For the connector, it is important to understand the effect of different gaps on its body. For the connector cable assembly, a test set-up was designed to identify and analyze the critical interfaces and derive a transfer function to predict the radiated field and validate with the measurements.

II. DVI COUPLING PATH ANALYSIS

To obtain an overview of the EMI, the system is tested inside a semi-anechoic chamber. The standard 3 m Federal Communications Commission (FCC) radiated field test shows the harmonics of the DVI spectrum that can cause the product to fail EMC certifications. For a given display resolution, the display driver clock operates at 148.5 MHz and the critical clock harmonics of 445.5 MHz and 742.5 MHz strongly show up in the radiated field tests with the fifth harmonic (742.5 MHz) only a few dB lower than the FCC class B limit, as shown in Fig. 3.

Fig. 4 illustrates certain unwanted gaps in the DVI system, which were individually examined to understand the different coupling paths.

For the DVI system, different coupling paths have been identified and their effects have been studied in the radiated field tests. The different coupling paths associated with each block mentioned earlier are shown in the coupling path diagram (Fig. 5). A method to interpret the coupling path

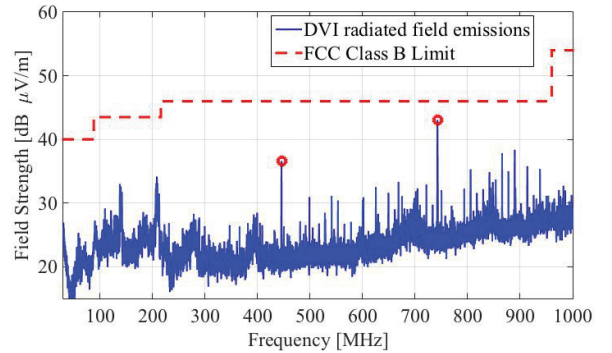


Fig. 3. Field strength at 3 m for DVI system.

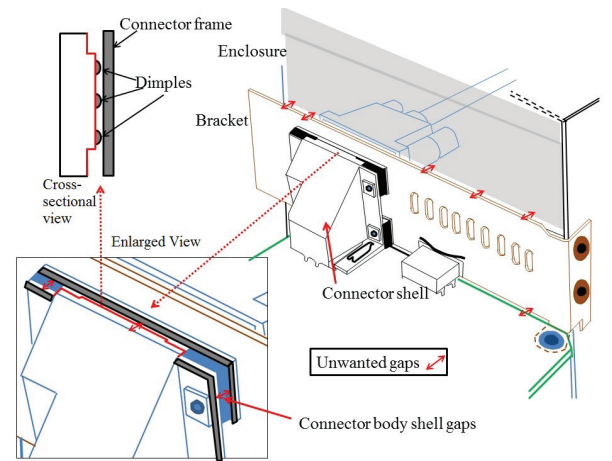


Fig. 4. DVI system showing unwanted gaps and imperfect contacts.

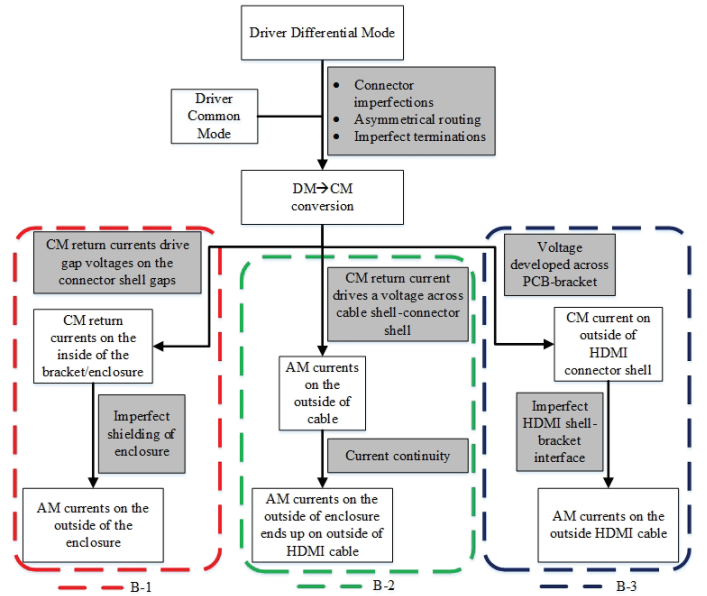


Fig. 5. DVI coupling paths.

diagram is to read the grey boxes between the connected boxes as the reason behind the mode conversion. From top-down, the coupling path states the different methods of the conversion from DM to CM in the system that return to the

source on the inside of the cable shield and connector shield. The three blocks after the DM to CM conversion describe the coupling paths on how the current path is disrupted and can appear on the outside as AM currents. Block B-1 refers to the connector body. Here, the CM return currents on the inside of the connector shell excite voltages on the connector shell gaps which drives currents on the inside of the bracket enclosure. This current appears as AM currents on the outside of the enclosure and cable as a consequence of an imperfect shielding of the enclosure (Fig. 4). An imperfect contact between the bracket and enclosure will have a voltage developed which in turn can drive AM currents on the outside of the metallic enclosure and cables. Block B-2 refers to the connector-cable assembly structures. Here, the CM return currents drive voltages at the different assembly interfaces (Fig. 2 at the interfaces: (A) DVI connector shell-DVI cable shell, (B) DVI connector shell-bracket, (C) bracket-enclosure) resulting in AM currents on the outside of the cable and enclosure. Similarly for block B-3; the AM current on the outside of the HDMI cable is a consequence of the imperfect shell of the DVI connector, the PCB bracket connection, and the imperfect contact at the HDMI shell-bracket interface.

A. Mode Conversion within the Connector Module

The different body shell gaps/apertures on a dual stack DVI connector are shown in Fig. 6. These gaps form the main coupling step to excite nearby structures such as an adjacent connector on the same PCB. For example, the seam between the top flange of the connector shell and the connector frame (Fig. 6 d) makes contact to the body frame of the DVI connector by three tiny tap points also known as dimples, through which the return current is constricted. The effect of such current confinement can be expressed by an equivalent inductance. These gaps need to be quantified using a meaningful metric that is reliable in determining the EMI performance of the connector. The connector transfer impedance is a parameter to judge the performance of such high-speed shielded connectors.

This transfer impedance relates the voltage across the connector shield gap/aperture to the CM return currents on the inside of the shield. To measure the connector transfer impedance, a test set-up was used and is shown in Fig. 7. The idea behind this set-up is to excite the connector in CM and measure the voltage across the gaps/apertures using an open coaxial probe. The measured S-parameters were then used to derive the transfer impedance for that gap. In this test set-up using a three port VNA, logical port 1 refers to the two balanced ports of the VNA which are used to excite the connector in CM while logical port 2 refers to the unbalanced single ended port of the VNA connected to the coax probe. This port mapping for the mixed mode S-parameter measurement is shown in Fig. 8. The transfer impedance is derived from the mixed mode S-parameter measurements and has been corrected for the probe impedance.

Here, it is important to analyze each gap in isolation, i.e., when voltage across (Fig. 6 d) is measured, all other gaps should be well connected. The gap under investigation

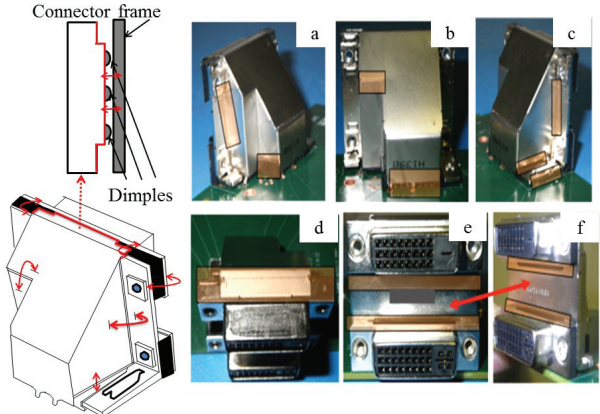


Fig. 6. Gaps on the DVI connector body.

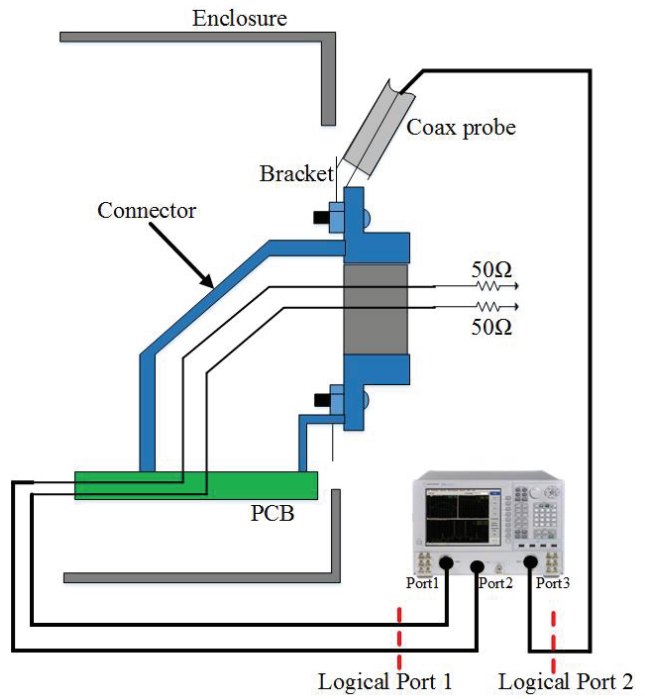


Fig. 7. Transfer impedance test set-up to measure $\frac{\text{slot voltage}}{\text{CM current}}$ dBΩ

was ensured to make no contact by inserting mylar tape between the contact points. All other gaps were well connected by copper tape. This method ensured the contribution was from the imperfect connection under investigation. Thus being able to investigate each gap in isolation. A higher transfer impedance value indicates a higher voltage is generated for the same amount of CM return current in the system. A higher voltage will drive higher AM currents, resulting in an increase in the emissions. Fig. 9 shows the measurement for two such gaps on the shell (position - a and position - d). The dynamic range on the plot refers to the port impedance range measured by measuring the impedance under open and short conditions. Getting the measurements in between the dynamic range indicates a successful measurement. From the transfer

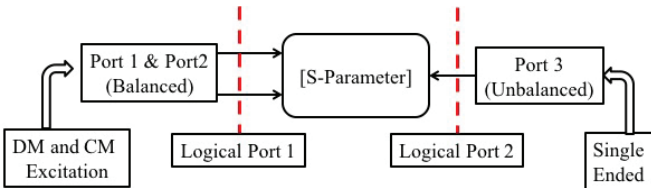


Fig. 8. Port mapping for 3 port mixed mode VNA measurements.

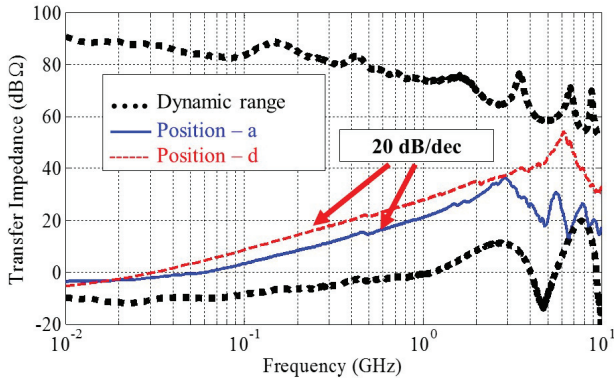


Fig. 9. Connector transfer impedance.

TABLE I
INDUCTANCE DERIVED FROM PORT IMPEDANCE MEASUREMENTS

	Inductance a linear region
Position a	1.98 nH
Position d	3.97 nH

impedance (Z_T) curves, an equivalent lumped inductance can be derived in the 20 dB/decade region from

$$Z_T = \omega L. \quad (1)$$

The extracted inductance (L) is assigned to each body shield gap. Table I lists the different inductance values.

Using transfer impedance as a metric, the most dominating gap on the connector body is determined; however, from an EMI design perspective, observing the impact of the dominating gap in radiated emissions is a more convincing test. For identifying the contribution of each slot towards the emissions, the radiated field was measured by making each gap imperfect in isolation. This ensured the contribution of only the gap under study. The test was performed on the actual system graphics card. Fig. 10 shows the test set-up. The graphics card with the connector under investigation was used to drive the monitor that is properly shielded under the table. A baseline was measured with the entire connector well shielded. Next, each slot was made imperfect one at a time and the field strength measured for each case. The measured field strengths were compared to the baseline case validating the transfer impedance results.

The top flange contact (Fig. 6 d) when made imperfect shows a maximum increase in field strength above the baseline

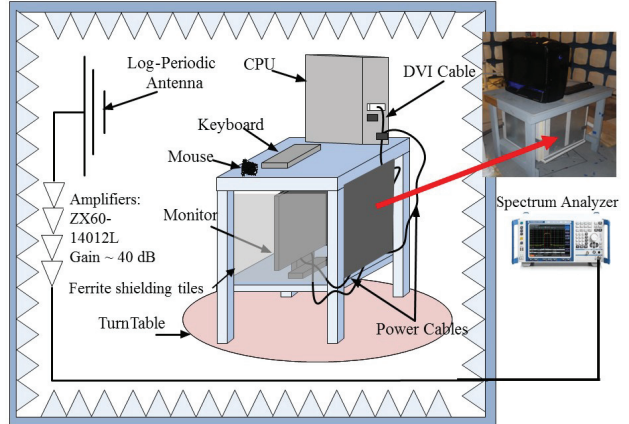


Fig. 10. Radiated field test setup.

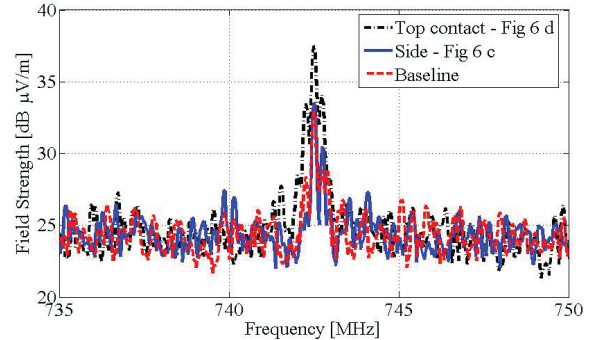


Fig. 11. Measured field strength around 742.5 MHz

TABLE II
FIELD STRENGTH FOR DIFFERENT CONNECTOR BODY SHIELDING AT 742.5 MHz

	dB μ V/m
Baseline	33.0
Top contact unshielded	37.6
Side unshielded	33.4

case. Fig. 11 shows the measured field strengths and Table II lists the field strength for each case.

Based on the above transfer impedance measurements, EMI performance of the connector shield was studied. Such quantification was the first step in the study of the overall performance of the DVI link system.

B. Cable shielding

It was important to study each of the connector-cable assembly structures in isolation in order to quantify their individual impact on EMI. The goal behind this test was to be able to measure the AM current on the DVI cable due to the different contact interfaces between the cable, connector, bracket, and enclosure. However, braided cables such as a DVI cable are known to show leakage through their own shields [12], [13], [14], [15]. This leakage would render the test set-up to fail as the AM measured on the cable shield would have a contribution from this distributed shield leakage. Hence, it

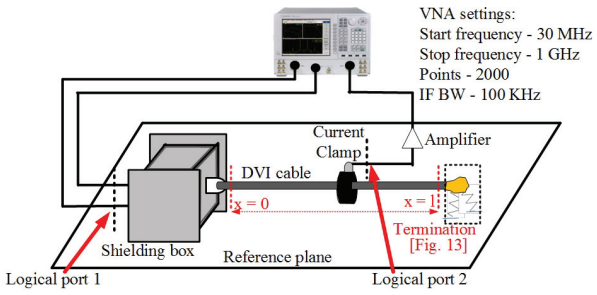


Fig. 12. Test set-up for cable shield leakage demonstration.

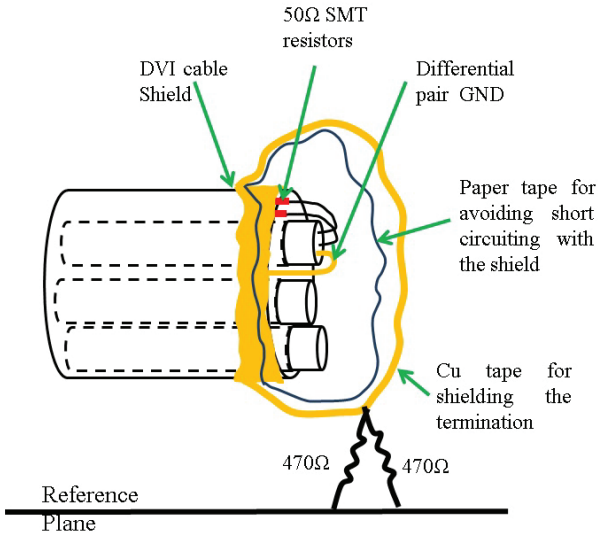


Fig. 13. DVI cable termination scheme.

was important to first identify if there was any shield leakage contribution from the DVI cable, remove this contribution, and then move to the next step of measuring the transfer function relating the driver DM excitation to the AM current on the cable.

Fig. 12 shows the test set-up for such a measurement. Port 1 and port 2 of the VNA are connected to one of the differential pair on the connector. The connector is located inside the shielding box. Port 3 of the VNA is used to measure the AM current using a current clamp through an amplifier. The current clamp was moved along the length of the cable and the AM current was recorded at intervals along the cable, starting from the connector end at $x = 0$ to the termination end at $x = l$ as indicated in Fig. 12. The signal lines of the DVI cable were terminated with a matched load of 50Ω to the shield of the DVI cable while the shield of the DVI cable was terminated via 235Ω to the reference plane as shown in Fig. 13.

The shield of the DVI cable forms a 235Ω transmission line with respect to the ground plane. To avoid reflections of the AM currents, two 470Ω resistances were connected in parallel to match the transmission line formed by the cable above a metal plate. This arrangement minimizes reflections.

Currents driven by connector gaps are distinguished from currents caused by shield leakage by observing the current distribution along the length of the cable. A current that is

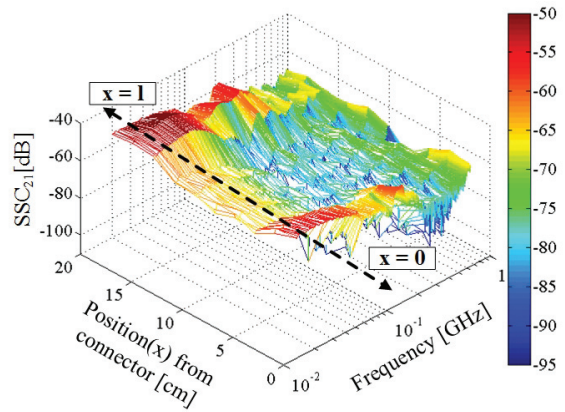


Fig. 14. AM current variation as a function of frequency and position showing distributed leakage.

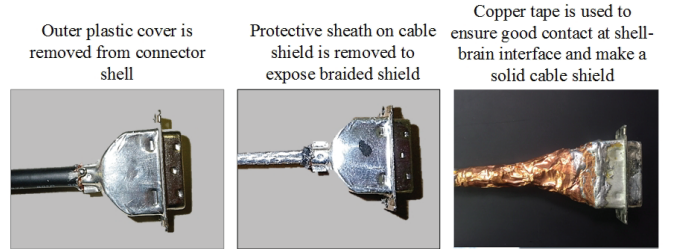


Fig. 15. Cable shielding process.

driven by a connector gap will have a constant magnitude from the connector to the termination as there is no reflected wave and no additional waves caused by leakage through the shield. However, distributed leakage will excite currents along the length of the DVI cable, thus leading to a fluctuating current magnitude along the length of the DVI cable.

By varying the current clamp location along the length of the cable, the conversion parameter (SSC_{21}) was measured from the connector end to the termination end. SSC_{21} refers to the current measured by the current probe (single-ended logical port 2) on the cable for a CM excitation of the connector (logical port 1). Fig. 14 shows this current (SSC_{21}) as a function of frequency and position.

By observing the current magnitude at a fixed frequency along the dotted line (from $x = 0$ to $x = l$), the strong variation that is explained by the distributed leakage was shown. Similar observations were made as the dotted line was swept along the frequency axis.

In order to isolate the AM currents on the cable due to the imperfect metallic connections from those caused by the distributed leakage of the cable, the DVI cable was modified as shown in Fig. 15.

The plastic cover around the cable shell and the outer protective sheath of the entire cable was removed. A 360° connection of the shield to the DVI cable connector shell was ensured using copper tape that was then extended to the entire length of the cable making a solid cable shield as compared to the previous braided cable shield. The same test was repeated using the cable with the modified solid shield. Fig. 16 shows

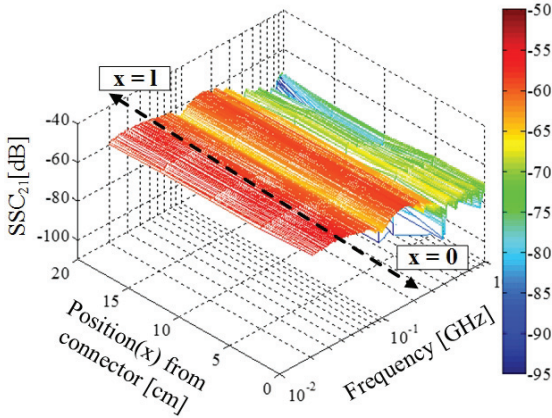


Fig. 16. AM current variation as a function of frequency and position of a solid shield cable.

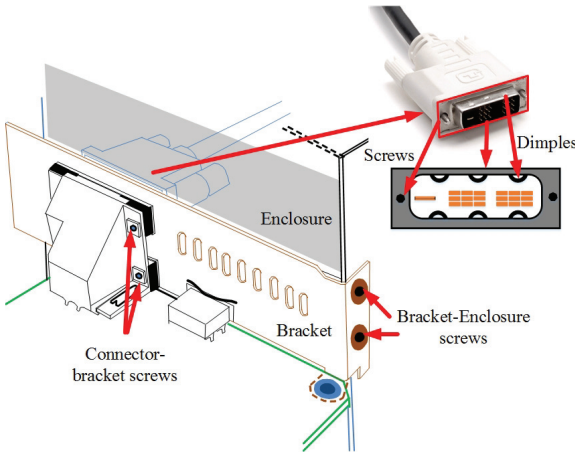


Fig. 17. DVI connector-cable assembly interfaces.

the same AM current measurement for the same cable with the modified solid shield. The same cable with the modified shield showed a uniform distribution of AM current along the position axis which is a consequence of the imperfect contact interfaces. With the shield leakage contribution removed from the test set-up, it was then used to measure the currents driven on the cable shield by the different imperfect contacts of the connector-cable assembly structures.

C. Connector-cable assembly

In this section the mechanical interfaces are dealt with, i.e., the cable shell interface, the bracket interface and the enclosure interface (as shown in Fig. 17). The connector shell and the cable shell were connected through six contact points called dimples, three on the top and three on the bottom, hence, it is not a perfect 360° connection.

Four screws, two screws on each DVI connector level, hold the DVI connector bracket together. Hence, this connection is also not perfect. Moreover, the bracket was fastened to the enclosure at one extreme end using only two screws.

The set-up in Fig. 18 was used to determine a transfer function which defines the ratio between the AM power

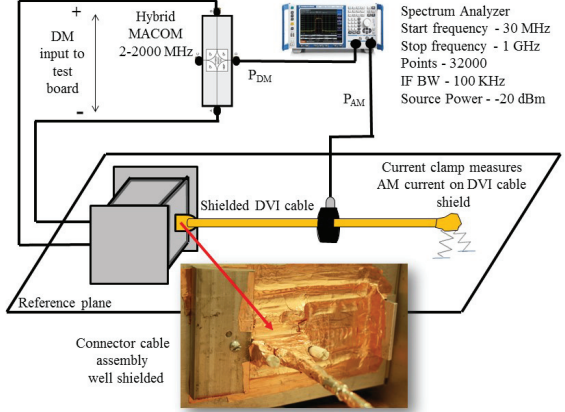


Fig. 18. Test setup for measuring the transfer function ($\frac{P_{AM}}{P_{DM}}$).

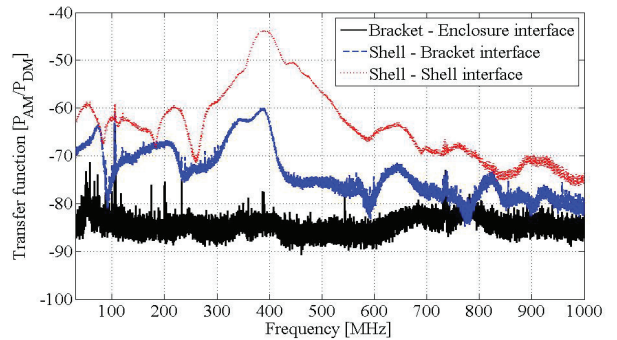


Fig. 19. Transfer function measured for different interfaces.

(P_{AM}) on the outside of the shielded DVI cable to the differential input power (P_{DM}) into the system ($\frac{P_{AM}}{P_{DM}}$). With the input differential power known, the antenna mode power was calculated and then converted to AM current to estimate the field strength for each case. For this measurement, a hybrid junction and a spectrum analyzer with tracking generator were used. The differential outputs of the hybrid are connected to one of the differential pair inputs of the connector test PCB. The idea behind this setup is to excite the connector system in DM and obtain the AM on the cable shield due to each imperfect contact in the system. This test was performed for the DVI connector.

Each case was analyzed individually by perfecting the shield of the other potential leakage contacts. The gap under study was made imperfect by adding mylar tape between the contacts while the other leakage gaps were well shielded using copper tape. Fig. 19 shows the measured transfer functions TF ($\frac{P_{AM}}{P_{DM}}$) for the different imperfect contacts (Fig. 2 A,B,C) measured one at a time. The data reveals that the shell-shell contact (Fig. 2 A) causes the strongest AM on the cable. For estimating the impact of these imperfect interfaces, the radiated fields needed to be estimated. The TF enables us to estimate the AM current's spectral density on the cable given a certain input DM power spectrum. The measured DVI DM spectrum is used as an input and the AM current on the cable is estimated for

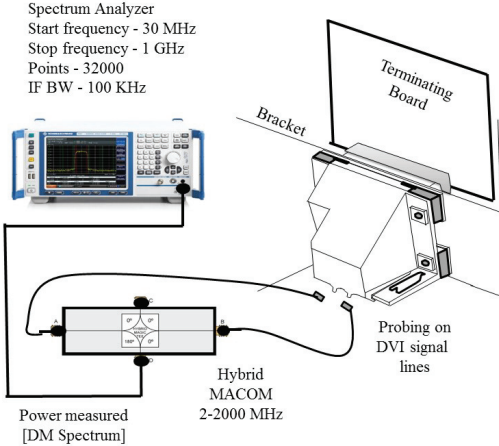


Fig. 20. Test set-up for measuring actual power supplied to the DUT - P_{DM} .

each case and the radiated emissions estimated and compared to the actual system emissions.

The power measured on the graphics card before the connector is used as (P_{DM}) input to the transfer function. Fig. 20 shows the measurement on the graphics card where the probes are connected before the connector by removing the DC blocking capacitors. Using this measured power spectrum, the AM current is calculated for the three cases. This AM current was then used as the current source in order to obtain the radiated field by using a simple dipole assumption [5], [16].

$$E = \frac{4\pi \times f I L \sin(\theta)}{r} \quad (2)$$

where, f - Frequency, I - Antenna-mode current, L - Length of cable, θ - Azimuthal angle, r - Observation distance.

An assumption in (2) is that a constant current flows along the entire length of the cable and it estimates the radiated field at a distance of 3 m from the wire.

For validating the estimation of the radiated field emissions, similar modifications were made on the connector-cable assembly on the actual system and the maximized radiated fields were measured in the semi-anechoic chamber. For example, the shell-shell interface was made imperfect using Mylar tape while all other gaps were properly shielded using copper tape. Fig. 21 shows the estimation around the DVI clock frequencies of 742.5 MHz and 445.5 MHz compared to the actual measured cases. The estimation is within ± 5 dB of the measured field values using the transfer function with an imperfect shell-shell interface.

III. CONCLUSIONS

A systematic methodology to quantify the EMI coupling within a DVI system is validated. This approach breaks the link from its source to the radiation into blocks that cause mode conversion and radiation. Each block is then individually analyzed. Based on the segmented transfer function approach the dominating imperfections in the DVI link are identified. To obtain the transfer function, a test set-up was designed to screen different cables based on their shielding performance.

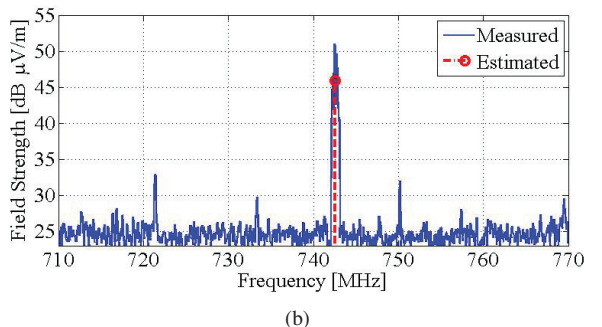
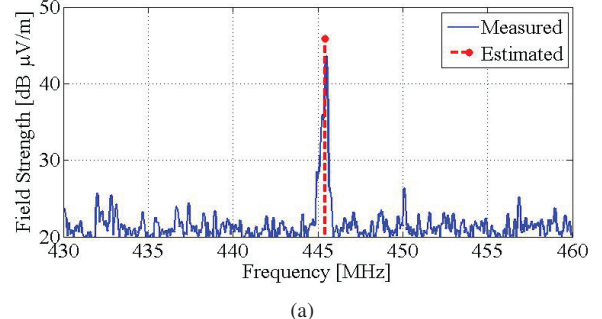


Fig. 21. Comparison of estimated field strength and measured field strengths at (a) 445.5 MHz; (b) 742.5 MHz.

The same set-up can be extended to other cable-connector systems as well, such as, HDMI, USB etc. The transfer function for the connector cable assembly along with the DVI source current can predict the critical emissions at 445.5 MHz and 742.5 MHz for radiated fields and was illustrated in this study. Using such a segmented model enables the designer to better understand the noise sources and estimate the EMI performance of the system without using computational heavy resources.

REFERENCES

- [1] *Digital Visual Interface DVI*, Digital Display Working Group, April 1999.
- [2] B. Archambeault, S. Connor, M. Halligan, J. Drewniak and A. Ruehli, "Electromagnetic Radiation Resulting From PCB/High-Density Connector Interfaces," *IEEE Transactions on Electromagnetic Compatibility*, vol. 55, no. 4, pp. 614–623, 2013.
- [3] *EMC Shielded Enclosures*, ELDON.
- [4] J. Kraemer and J. Shaw, "Achieving EMI Compliance with DVI and HDMI on Defense/Aerospace Platforms," in *IEEE International Symposium on Electromagnetic Compatibility*, 2009.
- [5] C. A. Balanis, *Antenna Theory: Analysis and Design*. Wiley, 2005.
- [6] K. Casey and E. Vance, "EMP Coupling Through Cable Shields," *IEEE Transactions on Electromagnetic Compatibility*, pp. 100–106, 1978.
- [7] Z. Hong-xin, L. Ying-hua, C. Shu-Liang and H. Yu-nan, "A Study on the Electromagnetic Leakage Arising from Braided Shielding Cable," in *Radio Science Conference, 2004 Proceedings, 2004 Asia-Pacific*, 2004.
- [8] *EMI Design Guidelines for USB Components*, Intel.
- [9] A. Clewes, "RFI/EMC Shielding in Cable Connector Assemblies," *Electronics & Power*, November 1987.
- [10] D. Hockanson, J. Drewniak, T. Hubing, T. Van Doren, F. Sha and M. Wilhelm, "Investigation of Fundamental EM1 Source Mechanisms Driving Common-Mode Radiation from Printed Circuit Boards with Attached Cables," *IEEE Transactions on Electromagnetic Compatibility*, vol. 38, no. 4, pp. 557–566, 1996.
- [11] A. Patnaik, Y. Zhang, S. De, D. Pommerenke, C. Wang and C. Jackson, "A method to quantify the coupling between DVI and HDMI connectors," in *2014 IEEE International Symposium on Electromagnetic Compatibility (EMC)*, 2014, pp. 289–294.

- [12] L. O. Hoeft and J. S. Hofstra, "Measured Electromagnetic Shielding Performance of Commonly Used Cables and Connectors," *IEEE Transactions on Electromagnetic Compatibility*, vol. 30, no. 3, 1988.
- [13] R. Tiedemann and K. Gonschorek, "Simple Method for the Determination of the Complex Cable Transfer Impedance," in *IEEE International Symposium on Electromagnetic Compatibility*, 1998.
- [14] R. Tiedemann, "Current Flow in Coaxial Braided Cable Shields," *IEEE Transactions on Electromagnetic Compatibility*, vol. 45, no. 3, pp. 531–537, 2003.
- [15] G. Zhou and L. Gong, "An Improved Analytical Model for Braided Cable Shields," *IEEE Transactions on Electromagnetic Compatibility*, pp. 191–163, 1990.
- [16] M. Aschenberg and C. Grasso, "Radiation from Common Mode Currents - Beyond 1 GHz," in *ESDEMC*, 2006.



James L. Drewniak (S'85-M'90-SM'01-F'06) received the B.S., M.S., and Ph.D. degrees in electrical engineering from the University of Illinois at Urbana-Champaign, Champaign, IL, USA, in 1985, 1987, and 1991, respectively. He has been a Professor of electrical engineering at the Missouri University of Science and Technology (former UMR), Rolla, MO, USA, since 1991. His research and teaching interests include signal and power integrity, electronic packaging, electromagnetic compatibility, and antenna design.



Abhishek Patnaik (S'10-M'15) received the B.E. degree in Electrical Engineering from the Institute of Technical Education and Research, India in 2010 and M.S. degree in Electrical Engineering from EMC Laboratory, Missouri University of Science and Technology, Rolla, MO, USA in 2015. He is currently working towards his Ph.D. degree in Electrical Engineering at EMC Laboratory, Missouri University of Science and Technology, Rolla, MO, USA. His research interests include On-Chip ESD, RF circuit design, EMC testing, grounding, and shielding techniques to improve electromagnetic compatibility.

Chen Wang photograph and biography not available at the time of publication.



Soumya De (S'07-M'13) received the B.E. degree in electronics engineering from Nagpur University, Nagpur, in 2007, and the M.S. and Ph.D degrees in electrical engineering from the Missouri University of Science and Technology, Rolla, MO, in 2008 and 2012 respectively. He is currently a Signal Integrity Engineer in the Core Hardware Group at Cisco Systems, San Jose, CA. His research interests include signal integrity, system architecture, PCB materials, electromagnetic compatibility, data fusion, nondestructive evaluation, and image processing.

Chuck Jackson photograph and biography not available at the time of publication.



Yao-Jiang Zhang (S'97-M'01-SM'11) received the B.E. and M.E. degrees in electrical engineering from the University of Science and Technology of China, Hefei, China, in 1991 and 1994, respectively, and the Ph.D. degree in physical electronics from Beijing (Peking) University, Beijing, China, in 1999. From 1999 to 2001, he was with a Post-Doctoral Research Fellow with Tsinghua University. From August 2001 to August 2006 and September 2008 to April 2010, he was a Senior Research Engineer and Research Scientist, respectively, with the Institute of High Performance Computing (IHPC), Agency for Science, Technology and Research (A*STAR), Singapore. From September 2006 to September 2008, he was with the Electromagnetic Compatibility (EMC) Laboratory, Missouri University of Science and Technology (formerly the University of Missouri-Rolla), Rolla, MO, USA, where he was an Associate Research Professor. He is currently with Huawei Inc., Shenzhen, China. His research interests include computational electromagnetics, electromagnetic interference and compatibility, signal/power integrity issues in high-speed electronic packages or printed circuit boards (PCBs), and photonic crystal and nanophotonic devices.



David Pommerenke (F'15) received the diploma degree and the Ph.D. degree in Electrical Engineering from the Technical University Berlin, Germany, in 1996. After working at Hewlett Packard for five years he joined the Electromagnetic Compatibility Laboratory, Missouri University of Science and Technology, Rolla, MO, USA, in 2001, where he is a Professor. He has published more than 200 papers and is inventor on 13 patents. His research interests include system level ESD, electronics, numerical simulations, and EMC measurement methods and instrumentations with focus on measurement/instrumentation ESD, and EMC. Dr. Pommerenke is an Associated Editor of the IEEE TRANSACTIONS ON ELECTROMAGNETIC COMPATIBILITY.